Key Engineering Materials Vol. 290 (2005) pp. 78-85
online at http://www.scientific.net

Failure Analysis on a De-NOx Catalyst of a Large Waste Burner

J. Kuebler [a], R. Baechtold, G. Blugan, K. Lemster, S. Fuso

EMPA, Laboratory for High Performance Ceramics, 8600 Duebendorf, Switzerland

[a] corresponding author: jakob.kuebler@empa.ch

Keywords: Waste burner, De-NOx catalyst, Failure analysis

Abstract: Modern waste burners are equipped with catalysts to reduce NO_X. During operation the catalysts and their performance are influenced by, for example rapid temperature changes, facility vibrations, cleaning procedures and unwashed exhaust gas (when the catalyst is installed before the washer). The catalyst discussed in this paper comprised over 2'500 extruded elements of 150 x 150 x 770 mm^3. During commissioning the catalyst elements exhibited a tendency to spall off pieces, thus preventing acceptance of the plant.
For the failure analysis, one element from the catalyst was removed and two spare elements were selected. The investigation comprised a visual check, fractography, measurement of the most important physical, mechanical and chemical properties, and a microstructural analysis. It could be shown that:

- Processing defects, such as extrusion defects, were the source of cracks which led to pieces spalling off;
- Hot steam, used for periodic cleaning, reduced the structural strength by half;
- The elements were exposed to higher mechanical loads than expected during transport;
- The cleaning process, in combination with particles transported by the exhaust gas, has an erosive effect on the catalyst material;
- Blockages, caused by catalyst material among other things, could be found at different depths;
- The chemical composition did not significantly differ between used and unused elements.

In summary, the failure analysis led to an understanding of the failure mechanism and to a set of recommendations for improvements whose implementation ultimately led to the plant being cleared for operation.

Introduction

NO_X is one of the critical toxic gases responsible for the so-called green house effect. In Switzerland, about 60 % of the overall amount of this gas comes from the transportation section. Secondary sources are small-scale combustion, industry, agriculture and waste (~ 5 %) [1]. This last contribution is not insignificant, and therefore, waste burners, which are mainly used to reduce the volume of the waste, should not only be equipped with electrostatic filters and gas washers to remove large and small particles from the incineration gas but also with a catalyst to reduce NO_X. Since commencement of a Clean Air Act (LRV) in Switzerland in 1991 the legal tool exists to enforce NO_X reduction in waste incinerators [2].

Different reduction techniques were developed in the 1980s, including selective catalytic reduction (SCR). Here, ammonia (NH_3) is added to the waste gas containing nitrogen oxides (NO_X), and the mixture is passed trough a catalyst layer. The NH_3 reacts selectively with NO_X according to Eq. 1, thereby reducing the toxic component to harmless nitrogen (N_2) and water (H_2O).

$$4\,NO + 4\,NH_3 + O_2 \xrightarrow{\text{Catalyst}} 4\,N_2 + 6\,H_2O \qquad (1)$$

In the case discussed here, a large catalyst of a waste burner started to fail due to pieces spalling off its elements even before the catalyst had passed the qualification test. An immediate replacement of the elements was out of question due to delivery times of up to several months. Of great concern was the fact that the catalyst was the first of a series of six which were to be installed in the same facility.

Experimental Procedure, Results and Discussion

Inspection of catalyst. It was decided to inspect the waste burner facility and catalyst in order to become familiar with the industrial waste burning process and the specific operating conditions, to gather failure relevant information, and finally, to propose an adequate investigation program as recommended in [3], for instance.

Waste burner facility. The waste burner facility comprised six burner lines which had to be retrofitted with catalysts to reduce NO_X. The catalyst discussed in this paper was the first to be installed in this retrofitting program. It was mounted between the electrostatic filter and the gas washer for better energetic efficiency, Fig. 1. (*Remark: A temperature of 270 °C is needed for the catalysis*). This position results in significant contamination of the catalyst by small particles not stopped by the electrostatic filter. At the time that the investigation was initiated, the catalyst had only been in operation for ~ 6'000 h, and this was not sufficient for successful approval.

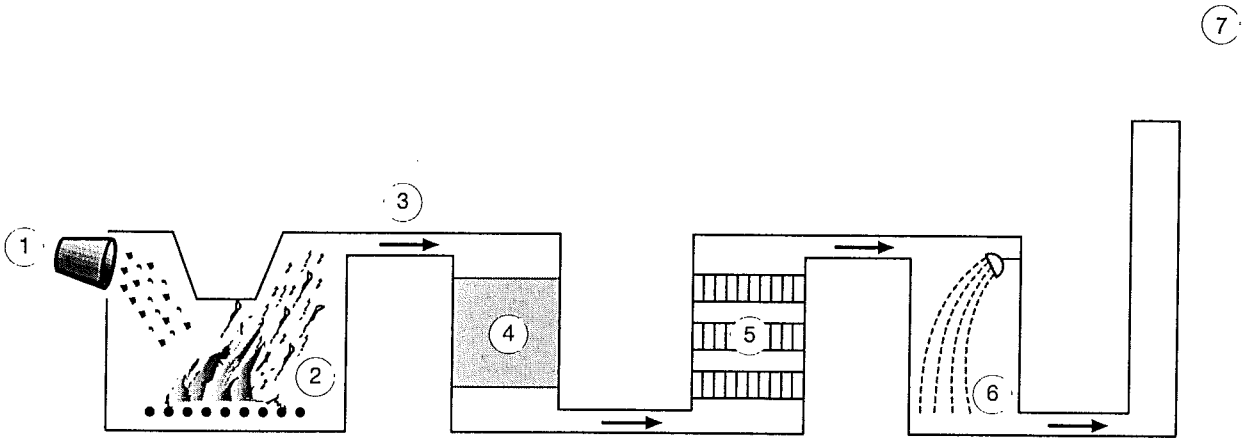

Fig. 1: Diagram of waste burner: 1) waste, 2) incinerator, 3) exhaust gas, 4) electrostatic filter for large particles, 5) NO_X catalyst with three layers of elements, 6) washer for small particles, 7) cleaned air.

Catalyst and elements. The catalyst contained three layers each consisting of 2 x 5 modules. The modules themselves were composed of 7 x 12 vertically-placed catalyst elements. Therefore, a total of 2'520 elements were mounted in this catalyst unit. The individual elements had a size of 150 x 150 x 770 mm^3 containing 40 x 40 channels. The free opening of the channels was 3.1 x 3.1 mm^2. The walls between the channels were ~ 0.6 mm. In total, the catalyst had an active surface area of nearly 20'000 m^2 (*or over 2.5 football fields*) not counting open porosity.

The elements were extruded from a feedstock containing ~ 70 wt% TiO_2 particles as the active catalytic component. The extruded elements were only dried (*not sintered*) and therefore had a green body like behaviour. After drying the elements were transported over 1'000 km by trucks equipped with air suspensions.

Cleaning and regeneration of catalyst. The position of the catalyst in the plant requires periodic cleaning and regeneration procedures to be performed. The cleaning procedure, which had already been carried out four times, is performed manually and its goal is to remove small particles which have collected on the channel walls. It contains the following steps:

- Cool down the catalyst from operating (~ 270 °C) to room temperature;
- Clean the catalyst manually with vacuum cleaners;
- Blow out the channels with compressed air (3.5 bars);
- Scrape off sticking particles by hand;
- Heat the catalyst to its operating temperature.

With the automated regeneration procedure which had been carried out three times, large salt particles which grow during operation are removed. The procedure contains the following steps:

- Clean with steam (6 bars) at operating temperature;
- Heat the catalyst to 310 °C and hold for 5 h;
- Cool down to operating temperature.

Visual inspection. The visual inspection of the catalyst revealed a large number of defects on the gas entrance and exit faces of elements. Typical defects were photographed and are shown in Fig. 2a and 2b.

Hypothesis of failure. After the visual inspection it was decided to continue the failure analysis based on the gathered information and on the following hypotheses:

- No defect pattern was detectable related to the layer sequence or exhaust gas entrance or exit faces;
- Elements had defects prior to operation;
- The size of the defects increased with increasing amounts of handling, transportation and operation;
- The cleaning or regeneration procedure degraded the structural integrity;
- The material was chemically stable and fulfilled its specifications.

Defect pattern. In a second detailed inspection, the gas entrance and exit faces of each element were assigned to a defect class. Having only 16 h for this task *(~ 10 s for an assignment)* defect classes were defined in advance based on the photographs taken during the initial inspection, Table 1. Further, to have a consistent definition of the defect criteria, a single person was committed for the assessments and someone else for collecting the decisions.

Table 1: Defect Classes

Class	Description
Class 1	Free of defects
Class 2	Spalled-off piece < ø 20 mm or a crack
Class 3	More than one defect of Class 2
Class 4	Spalled-off piece < ø 50 mm, see Fig. 2a
Class 5	Combination of defects of Class 2 and 4
Class 6	Spalled-off piece > ø 50 mm
Class 7	Combination of defects of Class 6 and 4 or 2, see Fig. 2b

Based on the collected data, a diagram for each gas entrance and exit face of the three element layers was drawn, e.g. Fig. 3. The diagrams showed no significant failure pattern. Therefore, it was concluded that the position of a layer or an element had no important influence on its defect class.

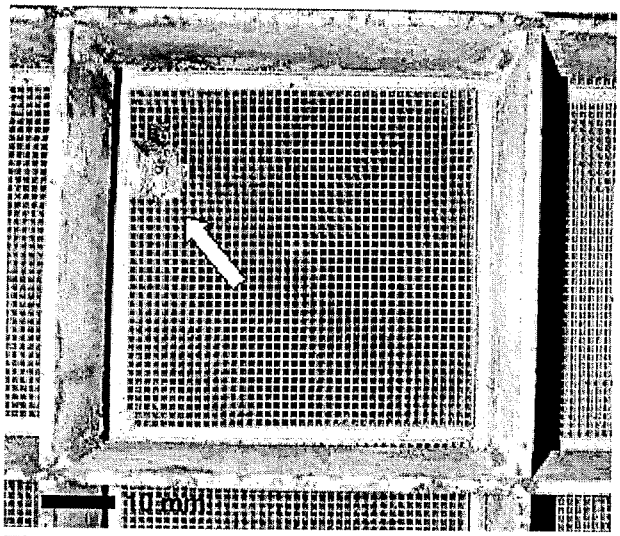

Fig. 2a: Gas entrance face of an element mounted on a support grid with a clogged up defect (arrow) defined as Class 4.

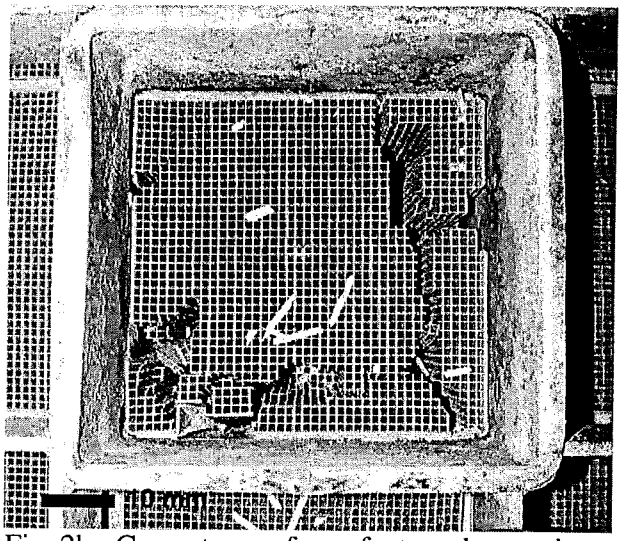

Fig. 2b: Gas entrance face of a test element in its metal casing with a defect defined as Class 7.

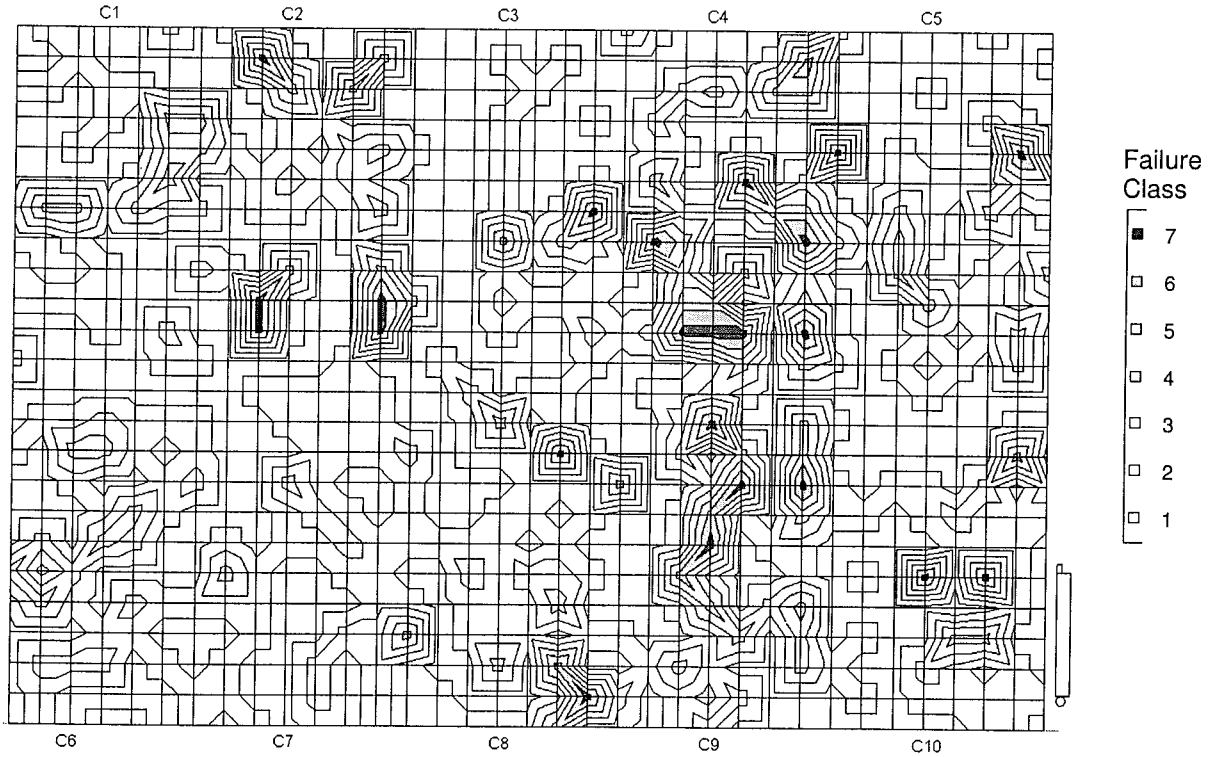

Fig. 3: Diagram for the visualization of defect patterns of a gas entrance or exit face of a complete catalyst element layer. White areas (elements) represent defect Class 1 (defect free) and black areas are rated Class 7. The notations C1 to C10 refer to the module number inside a layer.

Defects prior to operation. Three removable catalyst test elements together with their metal casing were selected for comparison and further analysis:

- Element A: Used element out of the middle layer, cleaned prior to removal;
- Element B and C: Unused elements.

Inspection of elements. Inspection of the elements after removing them from the metal casings revealed large defects on elements A and B, but only a small edge missing from C. On Element A,

pieces of various sizes had spalled off over almost the entire element length, Fig. 4a. Unused Element B exhibited cracking, with some cracks branching and running over almost its entire length, but no spalled-off pieces were visible, Fig. 5a and 5b.

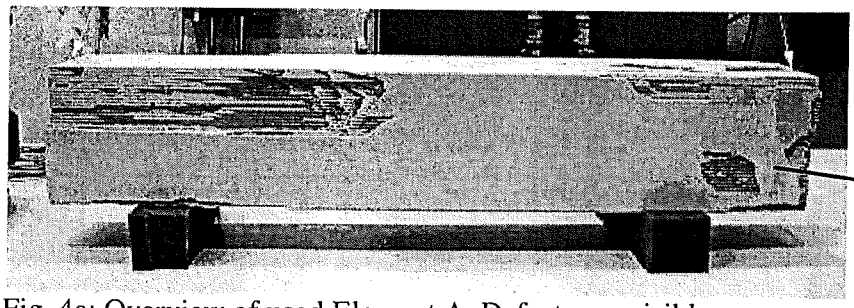

Fig. 4a: Overview of used Element A. Defects are visible over almost the entire length of ~770 mm.

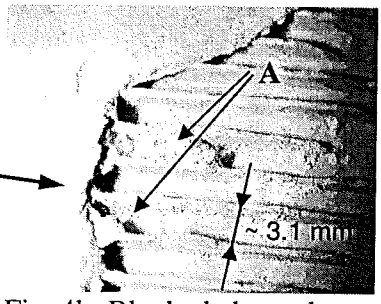

Fig. 4b: Blocked channels (arrow A) beneath spalled-off element skin.

Beneath a spalled-off skin area on Element A, blocked channels were visible, Fig. 4b. This defect could be a result of the cleaning or regeneration processes in which blocked channels are opened by compressed air 3.5 bars and steam at 6 bars.

It was noticed that the test elements were cushioned inside their metal casings with ceramic fibre bands fixed in place by tape, Fig. 5a. This kind of mounting is similar to the one of "normal" elements inside their module casings. Therefore, elements stored in a horizontal position experience a force like a bend bar simply due to their own weight. These forces are amplified when the elements are handled or transported. Bearing in mind that the elements are essentially green bodies and have a strength which is typically less than 10 MPa, as measured by Kuebler et al [4], this gives rise to the assumption that instantaneous or sub-critical crack growth due to drying, handling, transport, thermal, cleaning, and regeneration stresses started and enlarged the cracks.

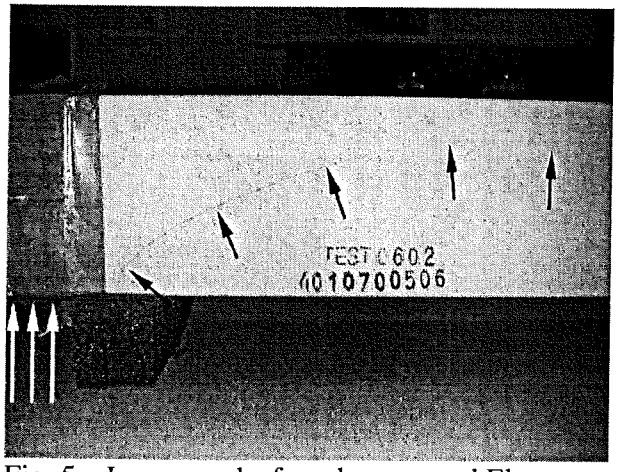

Fig. 5a: Large cracks found on unused Element B (black arrows). The white arrows mark the cushioning between the element and the metal casing.

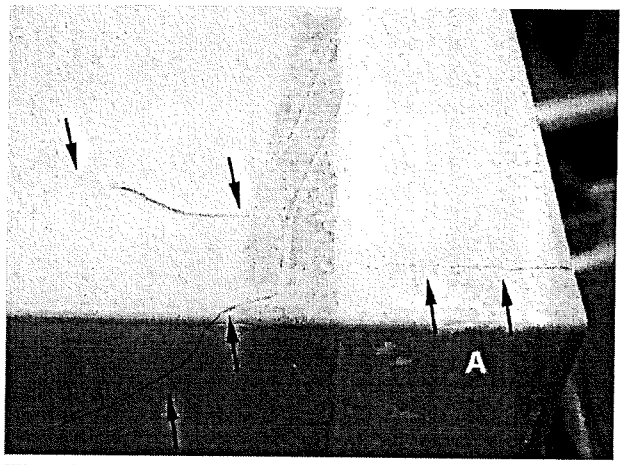

Fig. 5b: Crack starting at an element corner and branching after about 50 mm.

Verifying the specifications. For the elements, only the specific surface area and compressive strength were specified by the customer. To verify these specifications and prove some of the hypotheses, samples from the surface and core of the elements were removed to measure the density (He-Pycnometry), the specific surface area (BET), and the porosity (Hg-Intrusion). Table 2 shows that the specification for the specific surface area was fulfilled by both the used and unused

elements. The differences between the specific surface areas measured for the surface / core and used / unused elements may be a result of the small sampling volume and inhomogeneities in the material. On the other hand, the lower porosity measured on the surface of the used element may result from contamination by small particles from the unwashed exhaust gas.

Table 2: Physical Properties

		Spec.	Element A (used)		Element B (unused)		Element C (unused)	
			surface	core	surface	core	surface	core
Density	g/cm^3	--	3.7	3.7	3.6	3.6	3.6	3.7
Specific surface area	m^2/g	> 40	49	48	60	45	57	56
Porosity	vol%	--	38	50	52	53	50	52

Compressive strength of structure. The compressive strength of the element structure was specified with 0.7 MPa for cubes of size 150 x 150 x 150 mm^3. To verify this and to quantify the influence of the steam used during the regeneration procedure, four cubes were cut out of element C and compression tested under the following four conditions: relative humidity 41 % (*handling condition*), dried (*operating condition*), steam soaked, and dried / steam soaked / dried. The drying was conducted at 250 °C for 24 h in air and the steam soaking at 100 °C for 24 h at 100 % relative humidity. Under these conditions, Cube no. 4, for example lost 0.6 wt% during drying and gained 21 wt% when steam soaked due to filling up of the open porosity with water.

Drying the cubes revealed their high sensitivity to thermal stresses which, in one case, caused a large crack to develop, Fig. 6. This observation was interpreted as a high thermal shock sensitivity of the material / structure.

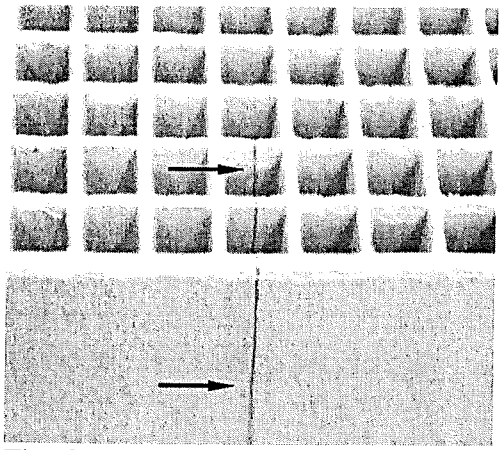

Fig. 6: Large crack in a cube caused by thermal stresses while drying.

Table 3: Compression strength

	Compressive Failure Strength [MPa]
Cube 1 (relative humidity 41%)	1.83
Cube 2 (dried)	2.31
Cube 3 (steam soaked)	1.14
Cube 4 (dried / steam soaked / dried)	1.77

Table 3 shows that drying a cube increases its overall strength by about 25 % and steam soaking decreases it to half of the dried strength. Further, it was shown that the strength after drying / steam soaking / drying is below the strength after simply drying, however, the structure still fulfils the minimal strength specified.

Extrusion defects. When cutting used Element A in half to remove samples for the physical property measurements, a significant extrusion defect almost 60 mm in diameter became visible, Fig.7. The effective dimension of the defect was even larger because the walls around became paper-thin due to an interruption of the feedstock flow during extrusion.

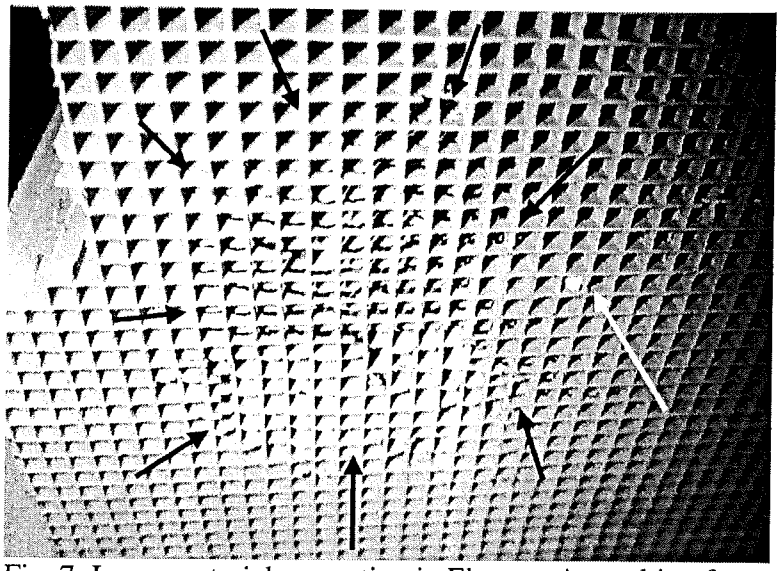

Fig. 7: Large material separation in Element A resulting from a feedstock flow interruption during extrusion (black arrows). The white arrow mark a blocked channel located almost in the centre of the element.

During inspection of failed elements from the compressive tests, many similar large defects were seen. Cracks started to grow from these defects first in the transversal and, after deflection, in the longitudinal direction, Fig. 8a. Additionally, small transversal cracks in channel walls were present, Fig. 8b. As stated earlier, the driving forces for starting and advancing cracks in unused elements are drying, handling, transport, and mechanical stresses.

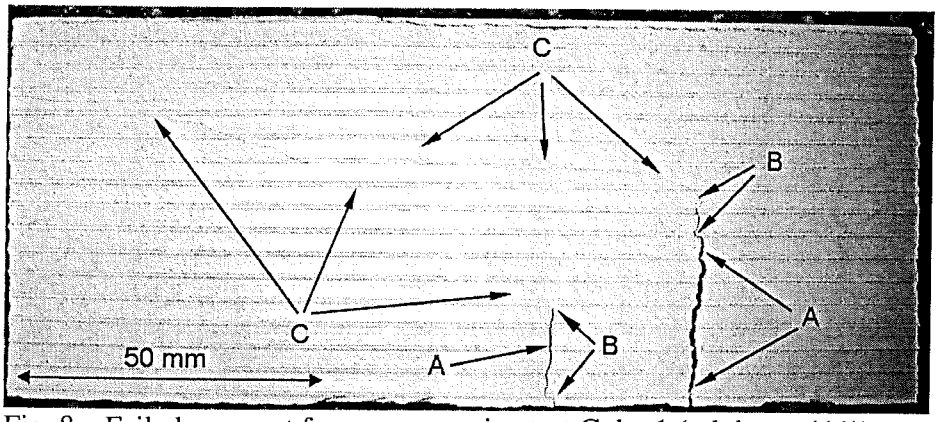

Fig. 8a: Failed segment from compressive test Cube 1 (rel. hum. 41%).
A) Defects due to interrupted feedstock flow during extrusion.
B) Cracks starting in transversal direction.
C) Cracks deflecting in longitudinal direction.

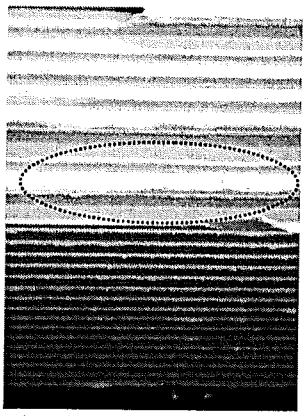

Fig. 8b: Small transversal cracks in channel wall of width 3.1 mm.

Microstructural and chemical analysis. To complete the failure analysis, microstructural (optical and scanning-electron microscopy) and chemical analyses were performed. SEM images showed that the cleaning process with hot steam, probably in combination with exhaust gas particles, has an erosive effect on the catalyst element structure. Further, it could be shown that micro-cracks are present in the channel walls of both the used and unused elements, Fig.9a and 9b.

Chemical analyses by X-ray diffraction (XRD) on used and unused catalyst material revealed no significant differences. Energy dispersive spectroscopy (EDS) analysis of channel obstructions like the one shown in Fig. 4b, showed sulphur, sodium, potassium, titanium, and silicon. The first three elements could not be detected in the unused element material, and therefore they must stem from

the exhaust gas. The fact that titanium and silicon were detected in the obstructions indicates that erosive removal and redeposition of the element material itself, helps to build up blockages.

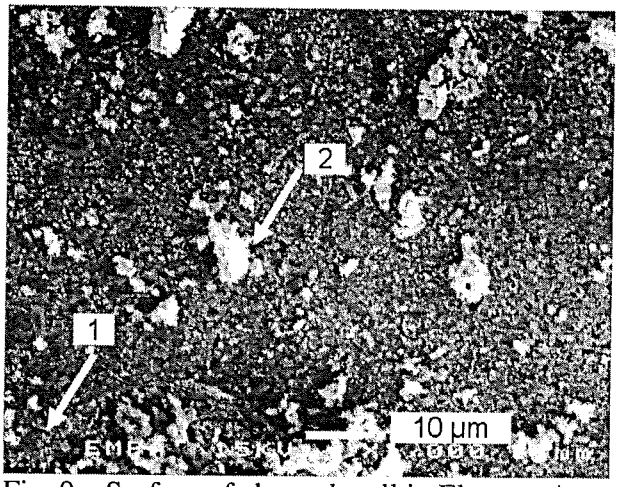

Fig. 9a: Surface of channel wall in Element A: 1) micro-crack; 2) particles from exhaust gas.

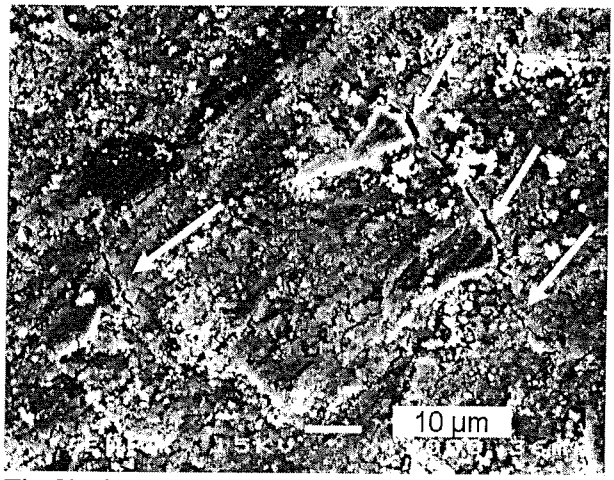

Fig 9b: Surface of channel wall in Element B. The arrows mark micro-cracks.

Conclusion

The main reason why pieces from the catalyst elements were spalling off was the significant number of large extrusion defects resulting from interruptions of the flow of the feedstock during extrusion. These defects are starting-points for cracks. Different driving forces, e.g. vibration during transport and thermal stresses during operation were responsible for further spontaneous and sub-critical crack growth, sometimes up to hundreds of millimetres in length.

Based on these findings, the following recommendations were made to improve fabrication, handling, and operation of the catalysts:

- Optimize the feedstock and extrusion process to eliminate extrusion defects which are the starting-points for cracks;
- Optimize handling and transport of the elements to suppress instant and sub-critical crack growth;
- Eliminate steam from the regeneration procedure because it reduces the structural strength by 50 % and can degrade strength permanently;
- Enlarge the cross-section of the channels to reduce the build up of blockages and make the walls thicker to increase the local strength of the structure.

Remark: After replacing the elements with improved ones and eliminating steam from the regeneration procedure, the catalyst passed the acceptance tests.

References

[1] Greenhouse Gas Inventory 1995, Second national communication of Switzerland 1997, Swiss Confederation, p36, http://unfccc.int/resource/docs/natc/swinc2.pdf

[2] „Clean Air Act of Switzerland", Luftreinhalte-Verordnung vom 16. Dezember 1985 (LRV), SR-Nummer 814.318.142.1, http://www.admin.ch/ch/d/sr/814_318_142_1/

[3] Technical Specification CEN/TS 843-6 Guidance for fractographic investigation, 2004

[4] J. Kuebler, F. Clemens, E. Aquino and T. Graule, Correlation between properties of extruded ZrO_2-rods in the green and as sintered state, CIMTEC 2002 – 10th Int. Ceramics Congress, Part A, Ed. P. Vincenzini, pp. 701-708, Techna Srl, 2003